Research Article

SURFACE and INTERFACE ANALYSIS

Received: 27 July 2007 Revised: 25 October 2007 Accepted: 1 November 2007 Published online in Wiley Interscience: 11 January 2008

(www.interscience.com) DOI 10.1002/sia.2664

New insights on the Cd UPD on Au(111)

M. C. del Barrio, S. G. García, C. E. Mayer and D. R. Salinas*

The Cd underpotential deposition (UPD) process on Au(111) was analyzed by means of combined electrochemical measurements and *in situ* scanning tunneling microscopy (STM). In the underpotential range 300 $\leq \Delta E$ (mV) $\leq$400, 2D Cd islands are formed on the *fcc* regions of the Au(111)-($\sqrt{3} \times 22$) reconstructed surface without lifting the reconstruction. At lower underpotentials, the 2D Cd islands grow and, simultaneously, new 2D islands nucleate and coalesce with the previous ones forming a complete condensed Cd monolayer (ML). STM images and long time polarization experiments performed at $\Delta E = 70$ mV demonstrate the formation of an Au–Cd surface alloy. At $\Delta E = 10$ mV, the formation of the complete Cd ML is accompanied by a significant Au–Cd surface alloying and the kinetic results reveal two different solid-state diffusion processes. The first one, with a diffusion coefficient $D_1 = 4 \times 10^{-17}$ cm^2 s^{-1}, could be ascribed to the mutual diffusion of Au and Cd atoms through a highly distorted (vacancy-rich) Au–Cd alloy layer. The second and faster diffusion process ($D_2 = 7 \times 10^{-16}$ cm^2 s^{-1}) is associated with the appearance of an additional peak in the anodic stripping curves and could be attributed to the formation of another Cd_zAu_x alloy phase.

Keywords: Au(111); Cd UPD; alloy formation; *in situ* STM

Introduction

The underpotential deposition (UPD) is an electrochemical phenomenon in which a metal can be deposited on a foreign substrate at a potential range that is more positive than the equilibrium Nernst potential of the 3D metal phase, and is produced by a strong interaction energy between the deposited metal and the substrate. The theoretical and experimental aspects of the UPD process were the subject of different reviews[1–8] and the formation of low dimensional metal phases, *i*D Me (with $i = 0, 1, 2$), during the UPD process has been intensively analyzed.[1,2,8] The formation of these *i*D Me phases is strongly influenced by surface defects like kinks, vacancies, chemical impurities, monatomic steps, stacking faults, etc.. In addition, in many UPD systems the strong metal–substrate interaction induces place exchange processes favoring surface alloying, which is more pronounced in systems exhibiting sufficient miscibility between the substrate and the deposited metal.[1]

Cd is known to produce intermetallic phases on Au during long-term polarization experiments in the UPD region.[9] Particularly, this UPD system has been the subject of several studies, some of them with contrasting results. By means of scanning tunneling microscopy (STM) and quartz crystal microbalance techniques,[10,11] the formation of different ordered adlattices during the Cd UPD in the system Au(111)/Cd^{2+}, SO_4^{2-} and the specific sulfate anion adsorption with underpotentially deposited Cd adatoms have been shown. Nevertheless, no information with regard to the surface alloy formation during the course of these experiments was indicated. The specific adsorption of sulfate anions during the Cd UPD on Au(111) was also suggested on account of specular X-ray reflectivity results.[12] It was demonstrated that the coverage of the Cd UPD layer increases with increasing sulfate anion solution concentration, but from these experiments the involved surface alloying was not clear. A surface alloy formation process was observed[13–16] in the system Au(100)/Cd^{2+}, SO_4^{2-} and it was concluded that, in this case, the Au–Cd surface alloy is formed during the UPD phenomenon probably by a turnover process between the adsorbed Cd atoms and the underlying Au atoms, with a subsequent solid-state diffusion of these atoms through the alloyed phase. The same mechanism was also proposed for the surface alloying observed during the Cd UPD on polycrystalline gold.[17] More recently, different authors[18–23] have determined that the Cd UPD is also possible on the reconstructed surface of Au(111) without lifting the reconstruction. They have also observed that Cd UPD results in some Cd atoms alloying with the Au atoms of the surface at potentials close to the reversible potential of the 3D Cd metal phase.

In this work new results of the Cd UPD in the system Au(111)/Cd^{2+}, SO_4^{2-} are presented, focusing on the Au–Cd alloy formation during this process.

Experimental

The experiments were carried out in the systems Au(111)/5 mM H_2SO_4 + 0.1 M Na_2SO_4 and Au(111)/1 mM $CdSO_4$ + 5 mM H_2SO_4 + 0.1 M Na_2SO_4 at a temperature $T = 298$ K. The electrolytic solutions were prepared from suprapure chemicals (Merck, Darmstadt) and fourfold quartz-distilled water. Prior to each experiment, the solutions were deaerated by nitrogen bubbling.

The working electrode was an Au(111) single crystal with a diameter of 0.4 cm. The surface was first mechanically polished with diamond paste of decreasing grain size down to 0.25 µm and subsequently electrochemically polished in a cyanide bath according to a standard procedure.[24] Electrochemical studies were performed in a standard three-electrode electrochemical cell

* *Correspondence to: D. R. Salinas, Instituto de Ingeniería Electroquímica y Corrosión (INIEC), Departamento de Ingeniería Química, Universidad Nacional del Sur, Avda. Alem 1253, (8000) Bahía Blanca, Argentina. E-mail: dsalinas@criba.edu.ar*

Instituto de Ingeniería Electroquímica y Corrosión (INIEC), Departamento de Ingeniería Química, Universidad Nacional del Sur, Avda. Alem 1253, (8000) Bahía Blanca, Argentina

at room temperature. A platinum sheet (1 cm^2) was used as a counter electrode and a $Hg/Hg_2SO_4/K_2SO_4$ saturated electrode (SSE) served as a reference electrode. The actual electrode potential, E, is referred to the SSE, whereas the underpotential, ΔE, is related to the Nernst equilibrium potential of the 3D Cd phase by $\Delta E = E - E_{3DCd}$, with $E_{3DCd} = -1150$ mV for $c_{Cd}{}^{2+} = 1$ mM. The measurements were carried out with a potentiostat–galvanostat EG&G Princeton Applied Research Model 273A.

The *in situ* STM images were recorded with a standard Nanoscope III equipment (Digital-Veeco, Santa Barbara, CA, USA) using Apiezon insulated Pt–Ir tips (Digital-Veeco, Santa Barbara, CA, USA). Pt wires were used as counter- and quasi-reference electrodes. The potentials of the gold substrate and the STM tip were controlled independently by a Nanoscope III-bipotentiostat optimized for the STM setup used. The tip potential was held constant at a value of minimum faradaic current and the tip current varied in the range $2 \leq I_{tun}$ (nA) ≤ 20. The experimental setup for the *in situ* STM technique has been checked by cyclic voltammetric measurements and the results were identical to those obtained in the conventional electrochemical cell.

Results and Discussion

Figure 1(a) displays a typical cyclic voltammogram obtained for the Au(111) surface in 5 mM H_2SO_4+0.1 M Na_2SO_4 solution. The anodic peak, A_r, observed at $E = -130$ mV corresponds to the lifting of the Au(111)-($\sqrt{3} \times 22$) surface reconstruction. This structure is stable in the potential range $E < -130$ mV.[25] In this potential range the STM images of the gold surface show flat terraces with the typical corrugation lines corresponding to *fcc* and *hcp* domains of the reconstructed surface[26] (Fig. 2). The lifting of this reconstruction is due to a disordered sulfate adsorption. In addition, the less pronounced anodic peak at $E = 410$ mV was assigned to the formation of an ordered sulfate adlayer.[27]

Figure 1(a) also shows a typical cyclic voltammogram for the system Au(111)/Cd^{2+}, $SO_4{}^{2-}$ recorded in the potential range $150 \leq \Delta E$ (mV) ≤ 1750. Two different adsorption–desorption current peak pairs are observed at $\Delta E_{A1/D1} \approx 650$ mV and $\Delta E_{A2/D2} \approx 350$ mV. The anodic peak A_r at $\Delta E = 1000$ mV ($E = -130$ mV) related to the lifting of the reconstruction is still present in the stationary voltammogram. This result is an evidence that the Cd UPD starts on the Au(111) reconstructed surface without lifting the reconstruction. By expanding the potential scan range up to the Nernst equilibrium potential of the 3D Cd phase (Fig. 1(b)), another current peak pair A_3/D_3 is observed. In this case, the anodic peak A_r is absent, indicating that the surface reconstruction would be, at least, partially removed when the Cd deposition is increased. Additionally, a distortion of the A_1/D_1 and A_2/D_2 peak pairs is also observed.

The surface morphology changes during the Cd UPD process were followed by *in situ* STM measurements. At $\Delta E \geq 800$ mV the STM images reveal no evidence of Cd deposition on the Au(111) substrate (Fig. 3(a)). The surface consists of atomically flat terraces separated by monatomic steps, and a few 2D gold islands. This surface morphology remains unchanged even in the underpotential range $450 \leq \Delta E$ (mV) ≤ 800 corresponding to the Cd UPD peak pair denoted as A_1/D_1. Different Cd expanded structures were reported on the reconstructed Au(111) surface in this underpotential region.[10,19] However, in the present study these expanded structures were not detected owing to a significant noise in the images, which reflects a high mobility in the

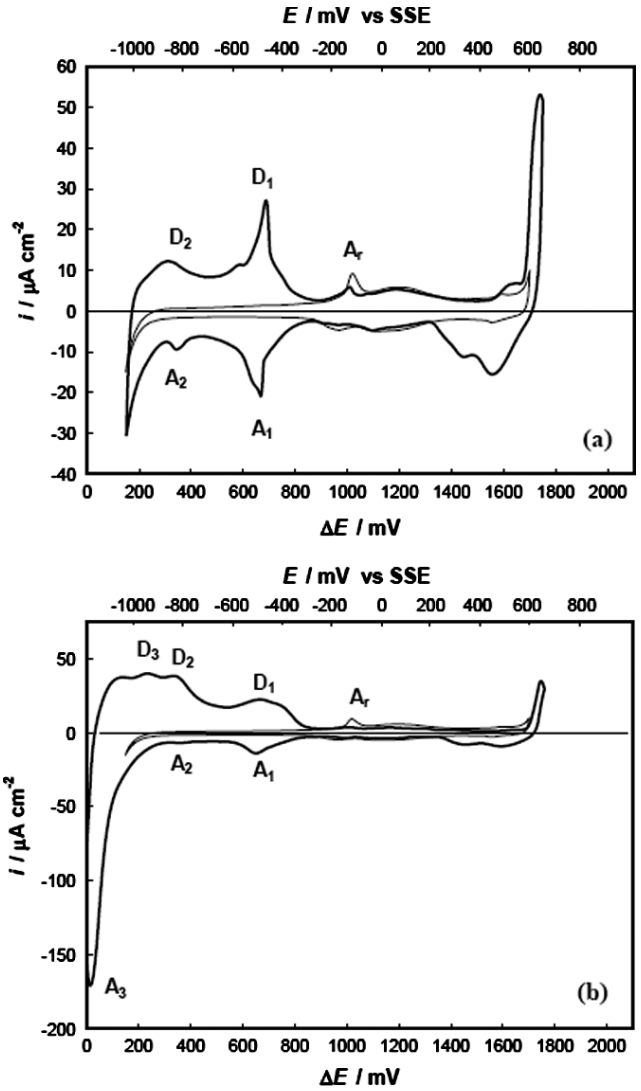

Figure 1. Cyclic voltammograms for the systems Au(111)/5 mM H_2SO_4 + 0.1 M Na_2SO_4 (———) and Au(111)/1 mM $CdSO_4$ + 5 mM H_2SO_4 + 0.1 M Na_2SO_4 (———) in the underpotential range: (a) $150 \leq \Delta E$ (mV) ≤ 1750 and (b) $0 \leq \Delta E$ (mV) ≤ 1750. $T = 298$ K, $|dE/dt| = 50$ mV s^{-1}.

adsorbate layer. At $\Delta E = 300$ mV, 2D Cd islands start to nucleate on the step edges and on the flat terraces (Fig. 3(b)). This process is related to the A_2 adsorption peak and could be ascribed to the occurrence of a first order 2D transformation of the expanded gas-like 2D Cd adlayer, observed by other authors at higher underpotentials, to a condensed Cd phase. When the potential is further scanned to cathodic direction the 2D Cd islands grow and, simultaneously, new 2D Cd islands nucleate (Fig. 3(c)) and coalesce with the previous ones. Consequently, the Cd deposits acquire linear chain morphology with 60° or 120° in between. This morphology is an indication that the underlying reconstructed Au(111) substrate is influencing on the deposition.[18,21,22] Similar results were also reported by Behm *et al.*[28] during the deposition of thin epitaxial Ni films at low overpotentials in the system Au(111)/Ni^{2+} and by Mao *et al.*[29] during the Sn UPD in the system Au(111)/Sn^{2+}. Mao and coworkers have indicated that an enhanced binding energy in the *fcc* region, and the fast diffusion of adatoms along the [11$\bar{2}$] direction favor the preferential nucleation

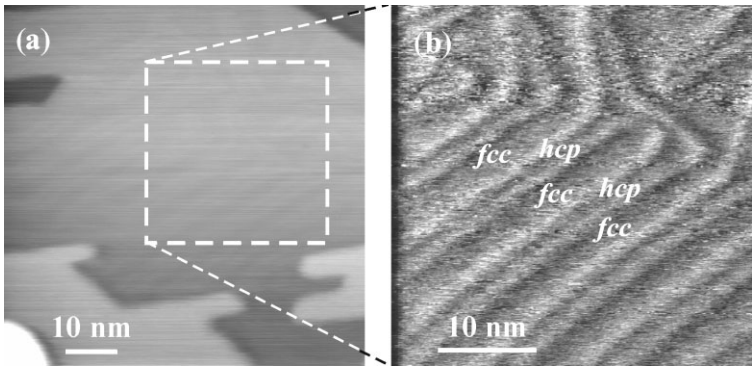

Figure 2. *In situ* STM images of Au(111) surface reconstruction. System: Au(111)/5 mM H_2SO_4 + 0.1 M Na_2SO_4, $E = -300$ mV. (a) substrate terraces ('height mode'); (b) high resolution image obtained in the area indicated in (a) ('current mode').

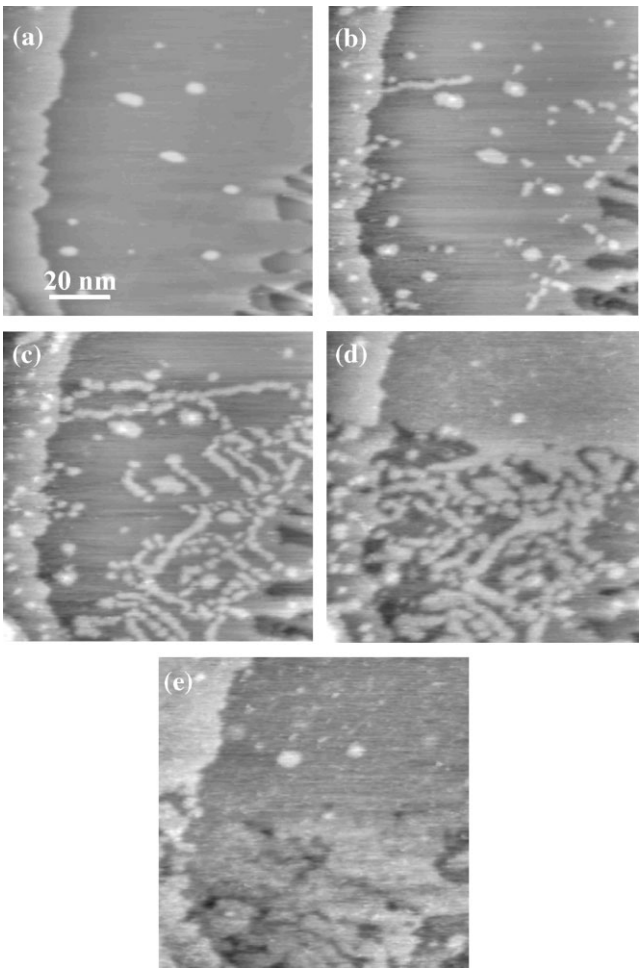

Figure 3. Sequence of *in situ* STM images obtained in the system Au(111)/1 mM $CdSO_4$+5 mM H_2SO_4+0.1 M Na_2SO_4, $T = 298$ K, at different polarization conditions. (a) $\Delta E = 900$ mV, (b) after 800 s at $\Delta E = 300$ mV, (c) after 350 s at $\Delta E = 150$ mV, (d) after 150 s at $\Delta E = 10$ mV, (e) after 200 s at $\Delta E = 10$ mV.

in the *fcc* region and, consequently, the anisotropic growth along the [11$\bar{2}$] direction.

At lower underpotentials, the Cd islands tend to merge forming a complete Cd monolayer (ML) (Fig. 3(d) and (e)). At this stage, the underlying gold surface is being probably reorganized as it is covered with Cd adatoms, which promotes that the subsequent Cd ML formed at $\Delta E \approx 0$ mV starts to grow without any axial preferences.[21] Obviously, the formation of an Au–Cd interfacial alloy in the underpotential range $0 \leq \Delta E$ (mV) ≤ 350 will contribute to this atomic rearrangement. The evidence of this alloying process is observed in the sequence of STM images showed in Fig. 4.

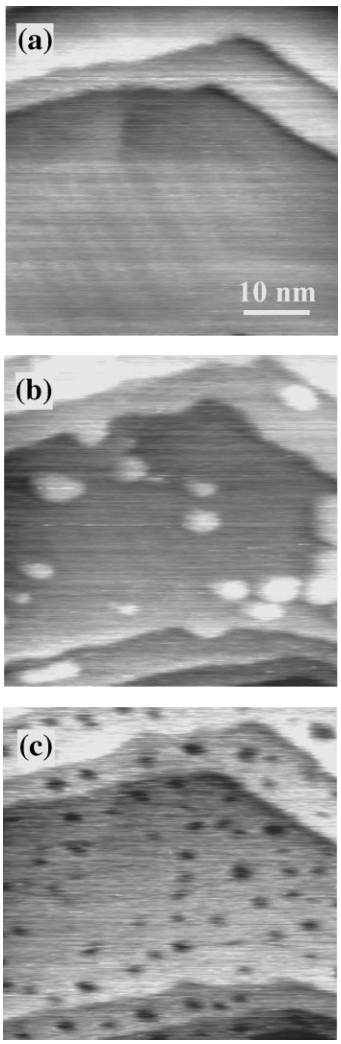

Figure 4. Sequence of *in situ* STM images obtained in the system Au(111)/1 mM $CdSO_4$ + 5 mM H_2SO_4 + 0.1 M Na_2SO_4, $T = 298$ K. (a) $\Delta E = 570$ mV; (b) after 40 s at $\Delta E = 70$ mV; (c) after 90 s at $\Delta E = 870$ mV.

By stepping the underpotential from $\Delta E = 570$ mV (Fig. 4(a)), where the formation of an expanded Cd adlayer takes place, to $\Delta E = 70$ mV, the nucleation of Cd islands on the *fcc* areas of the reconstructed surface is observed (Fig. 4(b)). Afterwards, when the underpotential is shifted positively to $\Delta E = 870$ mV, the Cd deposits are stripped and many holes of monatomic height are formed (Fig. 4(c)), which are typical for a surface alloy dissolution process.[13–15,18,19,30] The formation of this surface alloy could start at higher underpotential values, where Cd islands with linear chain morphology are formed,[18] probably following a place exchange mechanism between Cd atoms and Au surface atoms. Therefore, a 2D surface alloy could be formed at these regions, which would be the first step to the formation of a 3D Au–Cd alloy.

Long time polarization experiments were performed at low underpotentials in order to obtain information related to the Au–Cd alloy formation process. Figure 5(a) shows anodic stripping curves obtained after an extended polarization at $\Delta E = 70$ mV. The corresponding stripping charge density, Δq, increases gradually with increasing the polarization time, t_p, and the values are close to that required for the deposition of a complete close-packed Cd ML ($\Delta q_{mon} = 440\ \mu C\ cm^{-2}$) (Fig. 5(b)). Nevertheless, previous STM images (*cf* Fig. 4(b)) have indicated that the Cd ML is not complete at this underpotential value. Considering this observation and the presence of holes after the anodic stripping, it can be inferred that

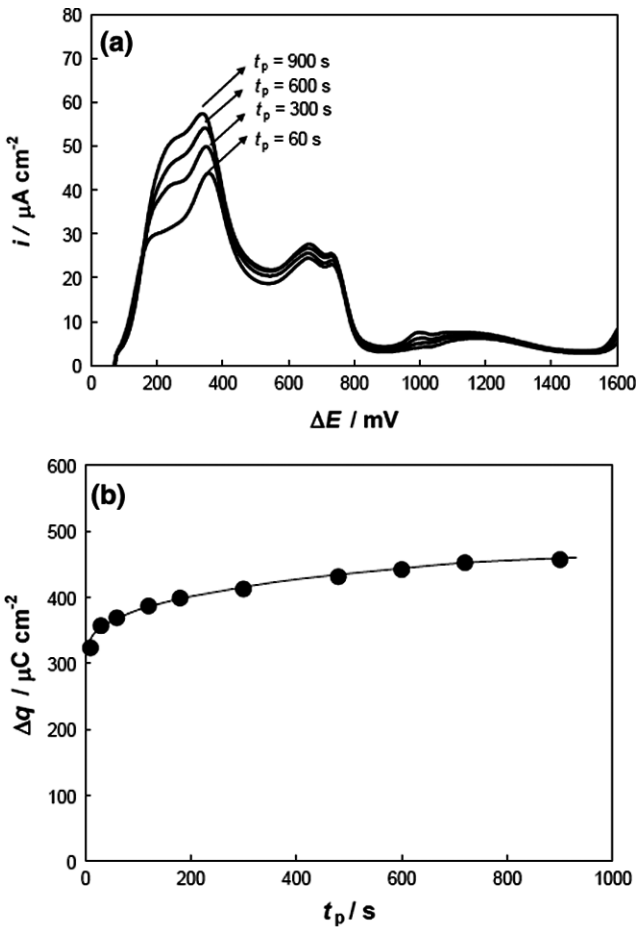

Figure 5. (a) Anodic stripping curves obtained in the system Au(111)/1 mM $CdSO_4$ + 5 mM H_2SO_4 + 0.1 M Na_2SO_4 after different polarization times, t_p, at $\Delta E = 70$ mV, $|dE/dt| = 50$ mV s^{-1}. (b) Corresponding stripping charge density Δq, as a function of the polarization time, t_p, at $\Delta E = 70$ mV.

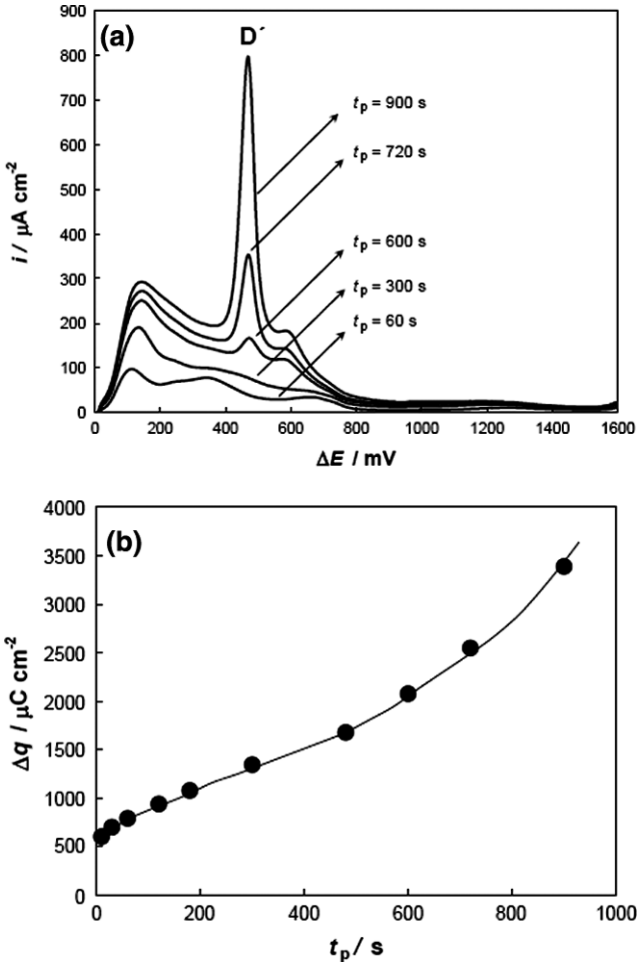

Figure 6. (a) Anodic stripping curves obtained in the system Au(111)/1 mM $CdSO_4$ + 5 mM H_2SO_4 + 0.1 M Na_2SO_4 after different polarization times, t_p, at $\Delta E = 10$ mV, $|dE/dt| = 50$ mV s^{-1}. (b) Corresponding stripping charge density Δq, as a function of the polarization time, t_p, at $\Delta E = 10$ mV.

a fraction of this charge is related to the formation of an Au–Cd surface alloy. Figure 6(a) shows the anodic stripping curves after an extended polarization at $\Delta E = 10$ mV. It is important to remark the appearance of an additional stripping peak D′ located at $\Delta E = 480$ mV for relatively long polarization times ($t_p \geq 600$ s). At this underpotential value, the STM images have shown that a complete Cd ML is formed. Nevertheless, the stripping charge density Δq, increases significantly exceeding that required for the deposition of a close-packed Cd ML (Fig. 6(b)). Experimental data presented in Fig. 7 display two different linear $\Delta q - t_p^{1/2}$ dependencies for relatively short and long polarization times. The parabolic dependence of Δq on t_p has been discussed previously in terms of a model including non-stationary mutual diffusion of Au and Cd in the Au/Au–Cd/Cd^{2+} system.[1,9] It has been suggested that the alloy formation process proceeds by mutual diffusion of Au and Cd atoms through a highly distorted (vacancy-rich) Au–Cd alloy layer and simultaneous Cd deposition at the Au–Cd/Cd^{2+} interface. According to this model, the stripping charge density can be expressed as: $\Delta q = \theta\ 2\ F\ c_0\ (D/\pi)^{1/2}\ t_p^{1/2}$ where θ is the coverage with respect to Cd at a given potential, c_0 is the Cd concentration at the electrode–electrolyte interface, D is the mutual diffusion coefficient, and F is the Faraday constant. Considering that the *in situ* STM images obtained at $\Delta E = 10$ mV

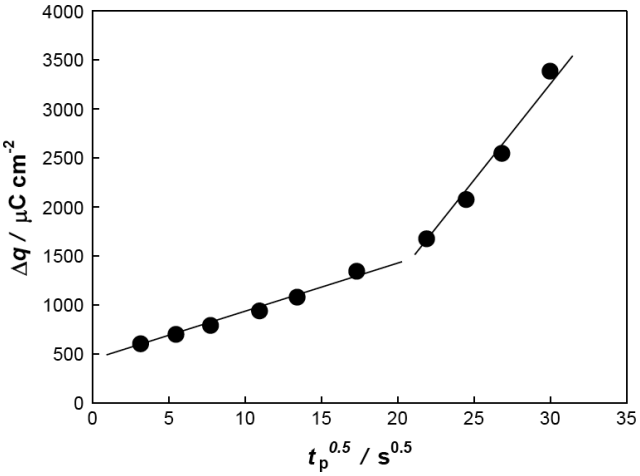

Figure 7. Stripping charge density Δq *versus* $t_p^{1/2}$ obtained for the system Au(111)/1 mM $CdSO_4$ + 5 mM H_2SO_4 + 0.1 M Na_2SO_4 at $\Delta E = 10$ mV.

have shown the formation of a complete Cd ML, a surface concentration of $c_0 = 0.0735$ mol cm^{-3} corresponding to a close-packed Cd ML could be assumed. From the initial linear $\Delta q - t_p^{1/2}$ dependence recorded at relatively short polarization times, a solid-state diffusion coefficient $D_1 = 4 \times 10^{-17}$ cm^2 s^{-1} is obtained. This value is close to that reported for the polycrystalline gold/Cd^{2+} system.[9,17]

The second $\Delta q - t_p^{1/2}$ dependence recorded at relatively long polarization times is coincident with the appearance of the additional D′ stripping peak and from the slope of this linear behavior, a solid-state diffusion coefficient $D_2 = 7 \times 10^{-16}$ cm^2 s^{-1} is calculated. A similar behavior was observed in the polycrystalline gold/Cd^{2+} system for relatively high cadmium coverage. In the present case, this faster solid-state diffusion process could be attributed to the formation of another Cd_zAu_x alloy phase evidenced by the presence of the additional stripping peak D′.

Conclusions

In the course of the Cd UPD process on Au(111), 2D Cd islands are formed on the *fcc* regions of the Au(111)-($\sqrt{3} \times 22$) reconstructed surface in the underpotential range $300 \leq \Delta E$ (mV) ≤ 400. At lower underpotentials, the 2D Cd islands grow and, simultaneously, new 2D islands nucleate and coalesce with the previous ones forming a complete condensed Cd ML. STM images and long time polarization experiments performed at $\Delta E = 70$ mV demonstrate the formation of an Au–Cd surface alloy. At $\Delta E = 10$ mV, the formation of a complete Cd ML is accompanied by a significant Au–Cd surface alloying and the kinetic results demonstrate two different solid-state diffusion processes. The first ones, with a diffusion coefficient $D_1 = 4 \times 10^{-17}$ cm^2 s^{-1}, could be ascribed to the mutual diffusion of Au and Cd atoms through a highly distorted (vacancy-rich) Au–Cd alloy layer. The second and faster diffusion process ($D_2 = 7 \times 10^{-16}$ cm^2 s^{-1}) is associated with the appearance of an additional peak in the anodic stripping curves and could be attributed to the formation of another Cd_zAu_x alloy phase.

Acknowledgements

The authors wish to thank the Universidad Nacional del Sur, Argentina, and the Agencia de Promoción Científica (PICTO-UNS 2004 Cod. 614) for financial support of this work. M.C. del Barrio acknowledges a fellowship granted by CONICET.

References

[1] Budevski E, Staikov G, Lorenz WJ. *Electrochemical Phase Formation and Growth*. VCH Verlag: Weinheim, 1996.
[2] Budevski E, Staikov G, Lorenz WJ. *Electrochim. Acta* 2000; **45**: 2559.
[3] Kolb DM, Przasnyski M, Gerischer H. *J. Electroanal. Chem.* 1974; **54**: 25.
[4] Kolb DM. In *Advances in Electrochemistry and Electrochemical Engineering*, vol. 11, Gerischer H, Tobias C (eds). John Wiley & Sons: New York, 1978; 125.
[5] Adzic RR. In *Advances in Electrochemistry and Electrochemical Engineering*, vol. 13, Gerischer H, Tobias C (eds). John Wiley & Sons: New York, 1984; 159.
[6] Szabó S. *Int. Rev. Phys. Chem.* 1991; **10**: 207.
[7] Leiva EPM. *Electrochim. Acta* 1996; **41**: 2185.
[8] Lorenz WJ, Staikov G, Schindler W, Wiesbeck W. *J. Electrochem. Soc.* 2002; **149**: K47, DOI: 10.1149/1.1519853.
[9] Schultze JW, Koppitz FD, Lohrengel MM. *Ber. Bunsenges. Phys. Chem.* 1974; **78**: 693.
[10] Bondos JC, Gewirth AA, Nuzzo RG. *J. Phys. Chem.* 1996; **100**: 8617.
[11] Niece BK, Gewirth AA. *Langmuir* 1997; **13**: 6302.
[12] Kawamura H, Takahasi M, Mizuki J. *J. Electrochem. Soc.* 2002; **149**: C586, DOI: 10.1149/1.1512671.
[13] Vidu R, Hara S. *Scr. Mater.* 1999; **41**: 617.
[14] Vidu R, Hara S. *J. Electroanal. Chem.* 1999; **475**: 171.
[15] Vidu R, Hara S. *Surf. Sci.* 2000; **452**: 229.
[16] Vidu R, Hara S. *Phys. Chem. Chem. Phys.* 2001; **3**: 3320.
[17] Inzelt G, Horányi G. *J. Electroanal. Chem.* 2000; **491**: 111.
[18] Lay MD, Stickney JL. *J. Am. Chem. Soc.* 2003; **125**: 1352.
[19] Lay MD, Varazo K, Srisook N, Stickney JL. *J. Electroanal. Chem.* 2003; **554–555**: 221, DOI:10.1016/S0022-0728(03)00183-9.
[20] Lee D, Rayment T. *Electrochem. Commun.* 2002; **4**: 832.
[21] Maupai S, Zhang Y, Schmuki P. *Surf. Sci.* 2003; **527**: L165, DOI:10.1016/S0039-6028(03)00078-5.
[22] Maupai S, Zhang Y, Schmuki P. *Electrochem. Solid-State Lett.* 2003; **6**: C63, DOI: 10.1149/1.1557035.
[23] Zhang Y, Maupai S, Schmuki P. *Surf. Sci.* 2004; **551**: L33, DOI:10.1016/j.susc.2003.12.017.
[24] Engelsmann K, Lorenz WJ, Schmidt E. *J. Electroanal. Chem.* 1980; **114**: 1.
[25] Kolb DM. *Prog. Surf. Sci.* 1996; **51**: 109.
[26] Barth JV, Brune H, Ertl G, Behm RJ. *Phys. Rev. B* 1990; **42**: 9307.
[27] Scherson DA, Kolb DM. *J. Electroanal. Chem.* 1984; **176**: 353.
[28] Möller F, Magnussen OM, Behm RJ. *Phys. Rev. Lett.* 1996; **77**: 3165.
[29] Mao B, Tang J, Randler R. *Langmuir* 2002; **18**: 5329.
[30] García SG, Salinas DR, Staikov G. *Surf. Sci.* 2005; **576**: 9, DOI: 10.1016/j.susc.2004.11.037.